A comparison of cellulose nanocrystals and cellulose nanofibres extracted from bagasse using acid and ball milling methods

M Rahimi Kord Sofla[1], **R J Brown**[1], **T Tsuzuki**[2] **and T J Rainey**[1]

[1] School of Chemistry, Physics and Mechanical Engineering, Science and Engineering Faculty, Queensland University of Technology, Brisbane, Qld 4000, Australia
[2] Research School of Engineering, College of Engineering and Computer Science, Australian National University, Canberra, ACT 0200, Australia

E-mail: t.rainey@qut.edu.au

Abstract

This study compared the fundamental properties of cellulose nanocrystals (CNC) and cellulose nanofibrils (CNF) extracted from sugarcane bagasse. Conventional hydrolysis was used to extract CNC while ball milling was used to extract CNF. Images generated by scanning electron microscope and transmission electron microscope showed CNC was needle-like with relatively lower aspect ratio and CNF was rope-like in structure with higher aspect ratio. Fourier-transformed infrared spectra showed that the chemical composition of nanocellulose and extracted cellulose were identical and quite different from bagasse. Dynamic light scattering studies showed that CNC had uniform particle size distribution with a median size of 148 nm while CNF had a bimodal size distribution with median size 240 ± 12 nm and 10 μm. X-ray diffraction showed that the amorphous portion was removed during hydrolysis; this resulted in an increase in the crystalline portion of CNC compared to CNF. Thermal degradation of cellulose initiated at a much lower temperature, in the case of the nanocrystals while the CNF prepared by ball milling were not affected, indicating higher thermal stability.

1. Introduction

Cellulose is the most abundant polymer in nature and has long been a major renewable source of materials [1]. Cellulose is a linear natural polymer of anhydroglucose units linked at the one and four carbon atoms by b-glycosidic bonds [2].

In plant cell walls, approximately 36 individual cellulose molecular chains connect with each other through hydrogen bonds to form larger units known as elementary fibrils or nanocellulose. These are further packed into larger microfibrils with a diameter of 5–50 nm and several micrometres in length. These microfibrils have disordered (amorphous) regions and highly ordered (crystalline) regions as illustrated in figure 1. The nanofibrillar domains, generally referred to as nanocellulose are a promising raw material for new bio based composites due to their high mechanical strength, stiffness, large surface area, low thermal expansion, optical transparency, renewability, biodegradability, low cost and low toxicity [3]. Potential applications based on these properties include their use as a reinforcing filler for polymers [4], mechanically adaptive nanocomposites [5], and flexible optical displays [6]. Apart from their use as a reinforcing filler for polymers, cellulose nanocrystals (CNC) and cellulose nanofibrils (CNF) have been used to fabricate a wide range of other functional
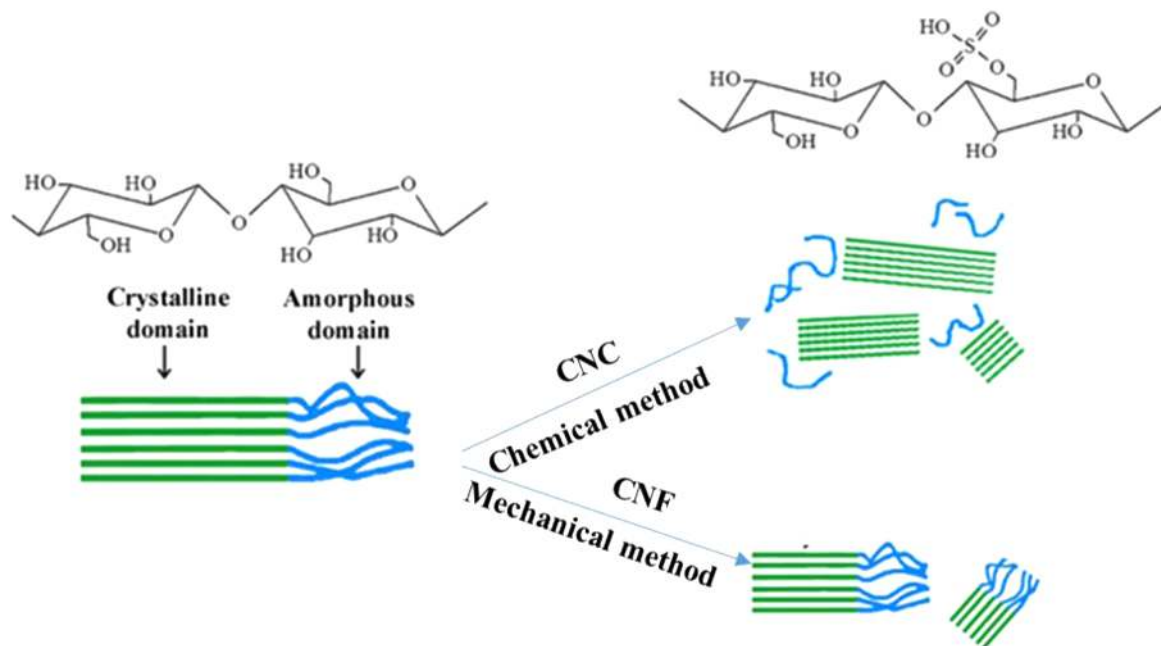
Figure 1. The mechanism of chemical and mechanical methods for producing CNC and CNF from cellulose.

materials, including transparent barrier films [7], photonic crystals [8], shape-memory polymers [9], drug carriers, composite materials [10], optical and electronic devices [11], and super capacitor electrodes [12].

Therefore, different techniques have been applied to produce nanocellulose. The nanofibrillar domains, generally referred to as nanocellulose, can be separated from each other by overcoming the extensive and strong inter-fibrillar hydrogen bonds with harsh chemicals, specific enzymes and/or intense mechanical forces.

When cellulose is subjected to pure acid hydrolysis treatment [13], the amorphous regions of cellulose micro-fibrils are selectively hydrolysed under certain conditions, as they are more susceptible to being attacked by acids in contrast to the crystalline domains. Consequently, these micro-fibrils break down into shorter crystalline parts with a high degree of crystallinity; these are generally referred to as CNC as shown in figure 1 [14].

Acid hydrolysis has been commonly used for CNC extraction from a great variety of sources, including: micro-crystalline cellulose [15], bacterial cellulose [16], cotton [17], wood [18], sisal [19], pineapple leaves [20], coconut husk fibres [21], bananas [22], wheat straw [23], pea hull fibre [24], branch-barks of mulberry [25], bagasse [26], bamboo [27] and ramie [28] because of its moderate operation conditions and the good stability of the resulting suspensions [29]. The nanocrystals have been reported to be either rod-like in shape (more commonly) or spherical [30]. CNC's geometry depends on the acid hydrolysis process conditions.

In contrast to CNC are CNF. Mechanical methods produce CNF together with the crystalline and amorphous regions by high shear forces. Different techniques have been employed to produce CNF, including high pressure homo-genisation [31], grinding [32] and ultrasonic techniques [33].

Ball milling is a top-down technique that forms micro to nano-scale materials, by inducing heavy cyclic deformation. Currently, ball milling is widely used for the preparation of nanoparticles because of its simple operation, use of relatively inexpensive equipment and its broad applicability to most types of biomass [34]. Another advantage over other mechanical treatments is that it easily produces nanocellulose in large quantities at room temperature and pressure.

Measurement of the fundamental properties of CNC and CNF is essential for understanding the relationships between structure and properties as well as processing conditions for a broad range of applications. In this paper, we report on the characterisation and comparison of CNC and CNF isolated from bagasse using both chemical and mechanical methods.

Although many lignocellulosic materials may be used to produce nanofibres, there is an important commercial economic advantage in using bagasse as a lignocellulosic fibre resource. The high cost of collection and transport, usually required for other lignocellulosic materials, is not required in the case of sugar cane bagasse. Sugar cane bagasse is centrally located at sugar mills, thus giving them an economic edge over other lignocellulosic fibres. It is a low value agricultural residue with 1.6 billion tonnes of bagasse (in 2011) being produced annually worldwide [35].

This study provides characterisation and comparison of CNF obtained by ball-milling with a more conventional CNC obtained via acid hydrolysis. The different forms of nanocellulose, are compared in terms of their chemical and crystalline structures, thermal stability, and morphologies.

2. Material and methods

Bagasse was obtained from a north Queensland sugar factory in Australia. Reagent grade chemicals used for fibre surface modifications and bleaching, namely, sodium hydroxide, potassium hydroxide, sodium chlorite and sulphuric acid were purchased from Sigma-Aldrich and used without further purification.

2.1. Isolation of chemically purified cellulose

For extracting cellulose, the bagasse was cut, ground and passed through a screen. The bagasse was then dewaxed with toluene-ethanol (2:1, v/v) in a soxhlet apparatus and then allowed to dry in an oven at 60 °C for 16 h. The dewaxed fibres were sequentially treated with 300 ml H_2O at 55 °C, to remove water-soluble components with the residue being filtered and washed until neutral pH. The residue was then delignified using acidified 1.3% sodium chlorite (acetic acid was used to reach pH 4). Finally the holocellulose was treated with 10% potassium hydroxide and 10% sodium hydroxide at 20 °C. After filtration, the cellulose was washed carefully with distilled water and 95% ethanol and dried in an oven for 16 h at 60 °C.

2.2. Extraction of CNC

CNC was isolated from sugarcane bagasse according to the acid-hydrolysis method [36]. In brief, the hydrolysis was performed using H_2SO_4 solution (64% w/w) at a ratio of 1:10 g ml^{-1} cellulose/H_2SO_4 at 45 °C for 60 min. After excess water was added, successive centrifugation was carried out at 12 000 rpm for 15 min to remove the acid and to stop the hydrolysis reaction. The remaining sulphuric acid was removed by dialysis until pH neutrality was reached. Then, the sample was sonicated for 10 min in an ice bath.

2.3. Extraction of CNC

CNF was produced using a Spex 8000M shaker mill. In a typical run, 0.25 g of bleached bagasse fibres were placed in a 70 ml polypropylene container along with 50 ml of deionised water and 20 g of cerium-doped zirconia balls (0.5 mm in diameter). The milling was performed for 1 h.

2.4. Characterisation

The surface morphology of CNF and CNC was examined using a Zeiss Sigma VP field emission scanning electron microscope (FE-SEM) with an accelerating voltage of 5 kV. Drops of CNC and CNF suspension (0.5% concentration) were deposited on carbon-coated electron microscope grids and dried at 45 °C then coated with a 10 nm gold layer.

The dimensions of the CNC and CNF were measured by transmission electron microscope (TEM). From the nano-cellulose suspension (4% w/v), 1 ml of the solution was dropped onto a 300 mesh nickel grid. After 2 min, the excess water was removed using a whatman no. 2 filter paper, and the grid was inverted and allowed to contact a drop of uranyl

acetate 2% (w/v) for 5 min. Finally, the grid was air-dried at room temperature for 24 h. The grid was analysed in a Morgani 268D TEM, with 0.2 nm resolution. The length and width of CNC and CNF were measured using the software Gatan DigitalMicrograph.

Energy dispersive x-ray spectroscopy (EDS) identifies the elemental composition of the sample. The EDS is a liquid nitrogen based 30 mm detector EDAX model. The EDS analyses are integrated characteristics of the SEM.

The chemical constituents of sugarcane bagasse and nanocellulose were investigated by FTIR spectroscopy using a nexus thermo FTIR (ThermoNicolet, USA) spectro-photometer. The FTIR spectrums of the samples were recorded in transmittance mode in the range of 400–4000 cm^{-1}.

The crystal structure was studied by x-ray powder diffraction measurements using a model XPert Pro Panalytical Diffractometer. The measurements were carried out with Cu Kα radiation at 40 kV and 40 mA. The crystallinity was calculated using equation [37, 38]

$$Cs = \frac{I_{002} - I_{am}}{I_{002}} \times 100, \qquad (1)$$

where Cs is the crystallinity (%), I_{002} is the intensity of (002) plane diffraction peak and I_{am} is the minimum intensity near the diffraction angle of 18.58 degrees.

Thermogravimetric analysis (TGA) of untreated bagasse fibre, extracted cellulose and acetylated cellulose was conducted in a temperature interval of 25 °C–600 °C under nitrogen atmosphere with a flow rate of 100 ml min^{-1} using an alumina crucible with a pinhole. A constant heating rate of 10 °C min^{-1} was maintained. A NETZSCH TG 209 F1 thermal analyser was used for the study.

Particle size measurements were carried out using dynamic light scattering using a Malvern 3000 Zetasizer Nano-ZS (Malvern Instruments, UK).

3. Result and discussion

3.1. Morphology of bagasse, cellulose, CNC and CNF

Figure 2 shows SEM micrographs of the original ground sugarcane bagasse at 100 μm scale (a) and at 10 μm scale (b); and extracted cellulose from bagasse (figures 2(c) and (d)). The original sugarcane bagasse consisted of fibrils of several microns. The smooth surface of the bagasse fibres is due to the presence of some non-fibrous components in the fibre surface such as lignin and waxes, pectin and oil. In figures 2(c) and (d), it is evident that the lignin and hemi-cellulose were removed through bleaching and the fibre bundles were separated into individual cellulose microfibres. Figures 2(e) and (f) show SEM and TEM of CNC produced by acid hydrolysis, respectively. The dimensions were calculated with the Gatan DigitalMicrograph software. The results showed that the CNC was needle-like in shape. They were uniform nano dimension bundles of crystals which are depicted in the TEM picture. CNC had size in the range of
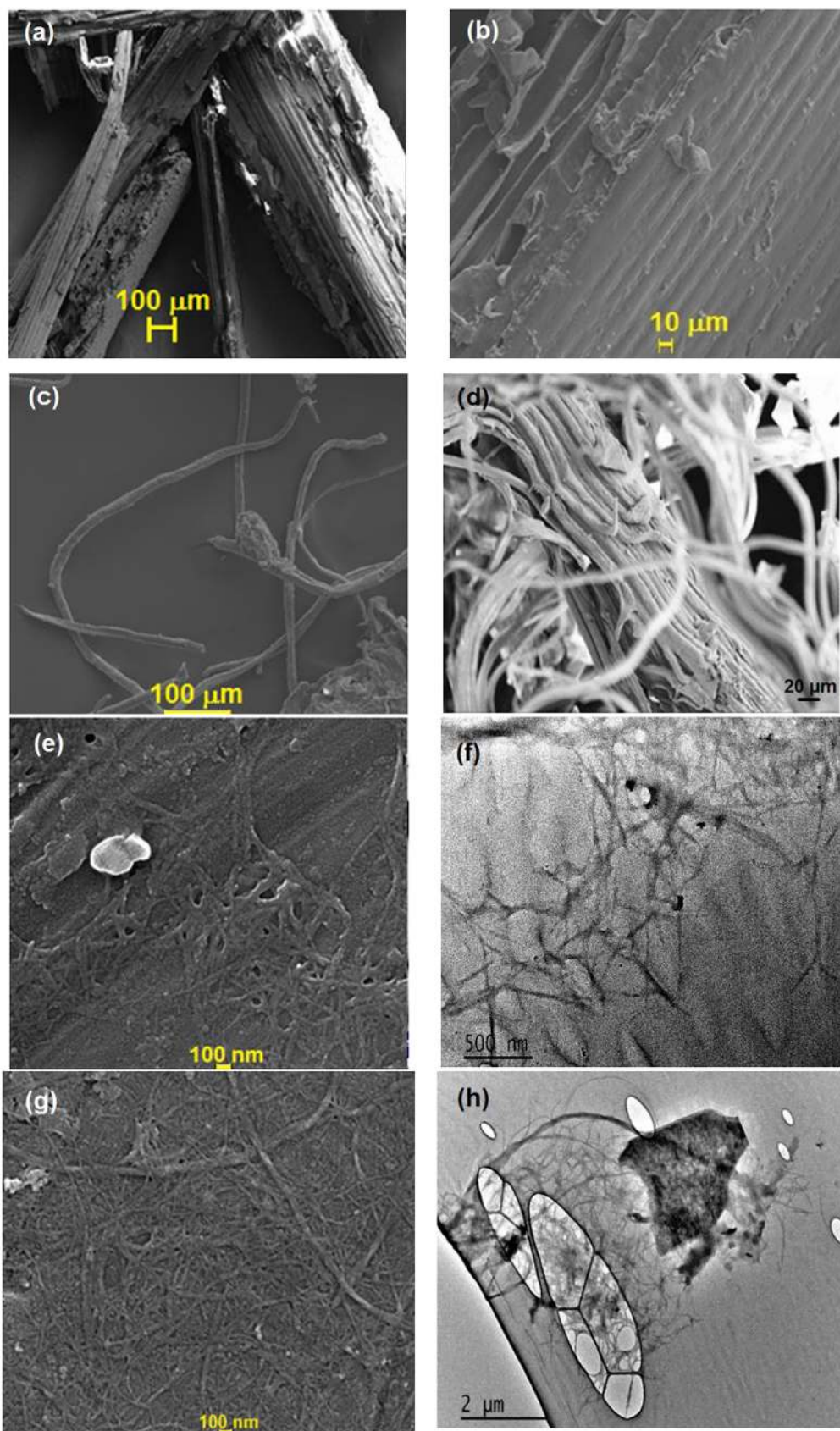
Adv. Nat. Sci.: Nanosci. Nanotechnol. **7** (2016) 035004

M Rahimi Kord Sofla *et al*

Figure 2. FE-SEM images of sugarcane bagasse as a raw material at (a) 100 μm scale and (b) 10 μm scale; extracted cellulose at (c) 100 μm scale and (d) 20 μm scale; CNF extracted by mill balling in (e) SEM and (f) TEM images; acid hydrolysed cellulose (CNC) in (g) SEM and (h) TEM images.
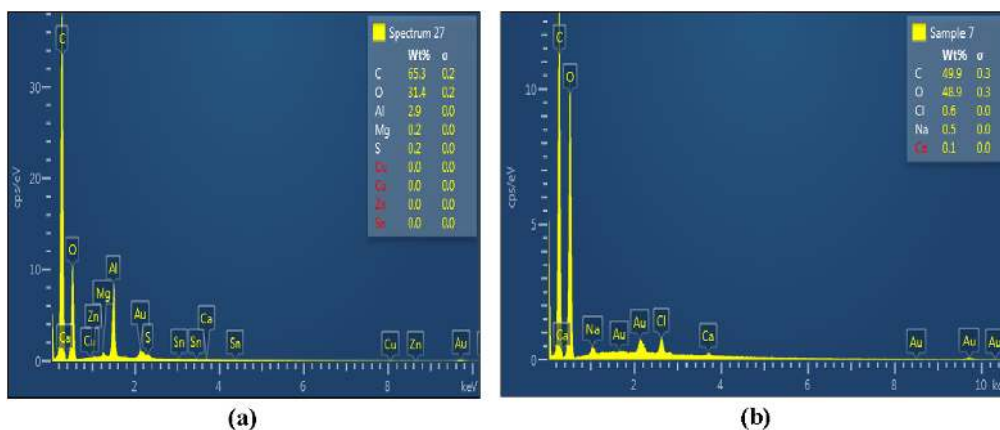
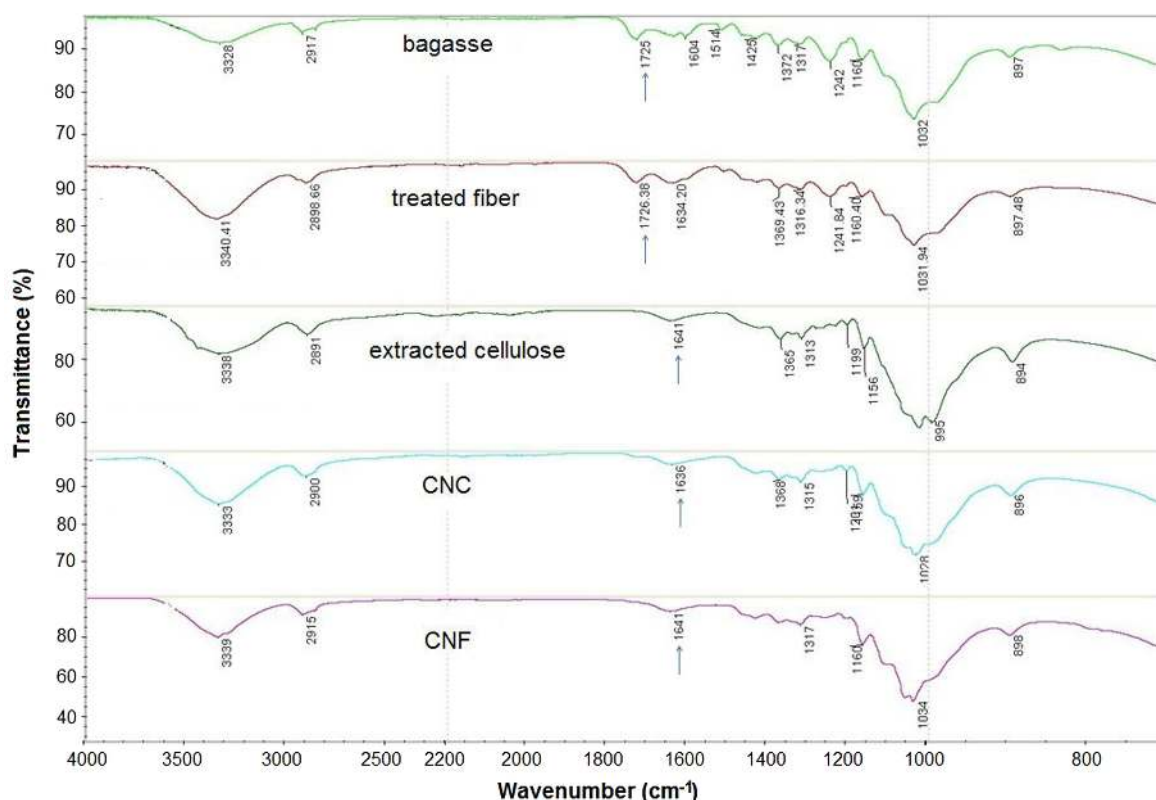**Figure 3.** Energy dispersive x-ray (EDX) diffraction for elemental analysis of (a) CNC and (b) CNF.

Figure 4. FTIR spectra of bagasse, treated fibres, extracted cellulose, CNC and CNF.

160−400 nm (length) and 20−30 nm (diameter) with a relatively low aspect ratio (11). Interestingly, for the CNF as seen in figure 2(g) SEM and 2(h) TEM produced by ball milling, had a length (L) of around 2000 nm and the diameters (D) of 50 nm, so had a higher aspect ratio (40) compared to CNC and were more rope-like in morphology.

3.2. Energy dispersive x-ray spectroscopy

Energy dispersive x-ray diffraction (EDX) attached with FE-SEM was used for elemental analysis of CNC and CNF. The EDX spectrum (figure 3) shows the peaks for carbon, oxygen and other elements corresponding to their binding energies. As expected, the two forms of nanocellulose possess mostly

carbon, oxygen and hydrogen. The amount of impurities is small. CNC contains 0.2 wt% sulphur impurity along with the main components: carbon 65.3% and oxygen 31.4% as shown in figure 3(a). CNF contains some sodium impurity (0.5%) resulting from a small amount of residual bleaching chemicals along with the main components: carbon (49.9%); and oxygen (48.9%) as shown in figure 3(b). The small amount of sulphur is due to the sulphuric acid.

3.3. FTIR analysis of the bagasse, cellulose, CNC and CNF

The FTIR spectra of sugar cane bagasse, cellulose, the CNC and CNF are shown in figure 4. Accordingly, all samples
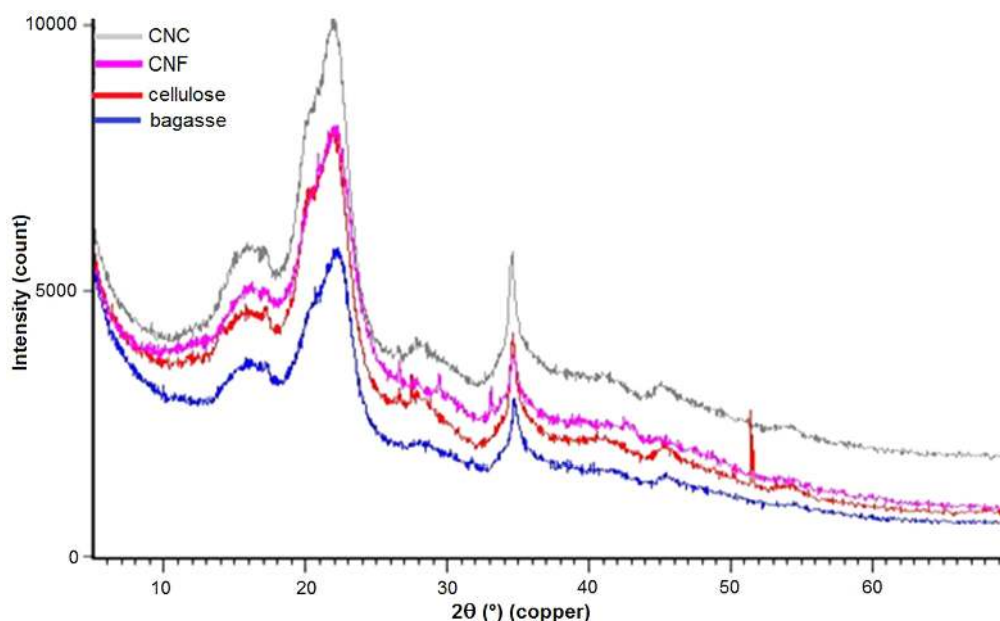
Figure 5. The XRD results of bagasse, cellulose, CNC and CNF.

presented two main absorbance regions in the range of 700–1800 cm^{-1} to 2700–3500 cm^{-1}.

The FTIR spectra of all samples have shown a wide band in the region between 3200 and 3500 cm^{-1} that specifies the free O–H stretching vibration of the OH groups in cellulose molecules [39]. The spectra of all samples showed the characteristic C–H stretching vibration around 2894 cm^{-1} [40]. In addition, the vibration peak detected at 1366 cm^{-1} in CNC and CNF samples is related to the bending vibration of the C–H and C–O bonds in the polysaccharide aromatic rings [41]. Alkali treatment reduces hydrogen bonding by removal of the hydroxyl groups through a reaction with sodium hydroxide. This led to the increase in –OH concentration, evident from the increased intensity of the peak between 3300–3500 cm^{-1} bands in all samples, compared to that of the untreated fibres in the figure. The peak centred at 1725 cm^{-1} in the FTIR spectrum of untreated sugarcane bagasse, and the faint peak at 1729 in delignified fibres, was mainly recognised due to the C–O stretching vibration of the acetyl and uronic ester groups; from pectin, hemicellulose or the ester linkage of carboxylic group of ferulic and p-coumaric acids of lignin or hemicellulose. Another possibility for this peak is that carboxyl or aldehyde absorption could have arisen from the opened terminal glycopyranose rings or oxidation of the C–OH groups [2, 42, 43]. Likewise, absorption peaks at 1604 cm^{-1} in untreated samples and was associated with aromatic C–C's in plane symmetrical stretching vibration of aromatic rings present in lignin [44]. These bands were no longer present in the FTIR spectra of cellulose fibres, CNC and CNF. The disappearance of these bands could have been caused by the removal of hemicellulose and lignin from bagasse fibres during the chemical extraction [45]. The spectrum of nanocellulose, however, resembles that of cellulose after delignification.

The absorbance peaks observed in the spectra of cellulose fibres obtained after treatment and the extracted CNF in the regions between 1641–1649 cm^{-1} were recognised by the O–H bending of the adsorbed water [2]. The slightly higher moisture content may be attributed to the absorption of moisture in the spaces left vacant from the removal of hemicellulose and lignin. The open surfaces created in the alkali treated cellulose helps absorb moisture. The higher moisture content for nanocellulose is probably due to the higher cellulose content.

Finally, the peak observed in the spectra of all samples between the 1025 and 1161 cm^{-1} range is due to the C–O–C pyranose ring (antisymmetric in phase ring) stretching vibration [46]. The most important absorption band that continually increases from bagasse to treated fibres and nanocellulose is at 902 cm^{-1} (associated with the glycosidic linkages between glucose units in cellulose).

The untreated bagasse fibres have a characteristic peak between 1600 cm^{-1} and 1730–1740 cm^{-1}. These peaks are mainly due to the hemicellulose and lignin components. These characteristic peaks are completely absent in the final cellulose and nanocellulose products therefore, cellulose and nanocellulose that are obtained by two different methods are effective in removing impurities, and the end product is free of hemicellulose and lignin.

3.4. X-ray diffraction of the bagasse, cellulose, CNC and CNF

The XRD graphs of the bagasse, cellulose and the CNF and CNC are shown in figure 5. The crystallinity was found to vary depending on the chemical and physical conditions applied. These samples showed typical cellulose I structure with a wide peak around $2\theta = 16.5°$, 22.5° and 34.6° [47].

The crystallinity of bagasse, cellulose, CNF and CNC was calculated to be 45%, 65%, 68% and 73%, respectively.
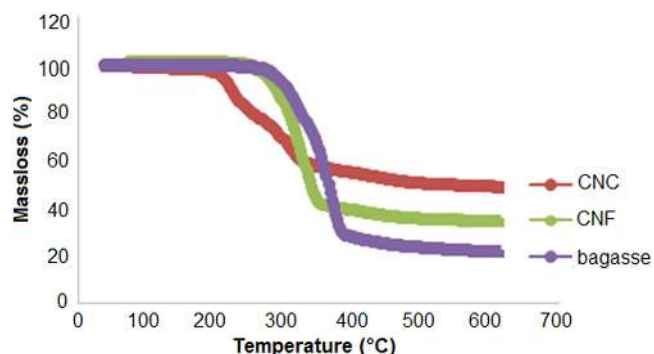
Figure 6. Analyses of sugarcane bagasse, CNC and CNF via TGA.

The non-treated bagasse fibres were less crystalline than the treated ones. The higher intensity peak associated with CNF, CNC and cellulose is due to the removal of amorphous components with the consequent increase in the cellulose index [44]. Considering that hemicellulose has a random, amorphous structure, the samples of cellulose, CNF and CNC have little or no hemicellulose present. The maximum crystallinity was obtained with CNC. In the process of hydrolysis, the hydronium ions penetrated the amorphous regions of the cellulose, promoting the hydrolytic cleavage of glyosidic bonds and finally releasing the individual crystallites [48, 49].

Ball milling does not have a negative effect on the crystallinity. There is not a remarkable difference in the XRD patterns between CNC and the CNF. The small change in crystal structure and the crystallinity of CNF is similar to the results of Amiralian and co-workers [50]. Their results confirmed that mechanical treatment by ball milling does not have a negative effect on the crystallites of cellulose compared to the ultrasonication method.

3.5. Thermal analysis

TGA curves for bagasse, CNC and CNF obtained via conventional sulphuric acid treatment and the ball milling treatment methods are provided in figure 6. The initial weight loss of approximately 4% is due to the evaporation of loosely bound moisture on the surfaces of these materials in the graph. The chemisorbed water or the intermolecular H-bonded water (as apparent from the characteristic peak of FTIR spectra at 1649 or 1641 cm^{-1}) was found to be given off at 120 °C [51–53].

Further loss in weight may be attributable to pyrolysis; pure bagasse was observed to decompose in the 319 °C– 378 °C region whereas CNF decomposed at a slightly lower temperature (299 °C–364 °C). The lower degradation temperature of CNF could be due to the smaller fibre dimensions compared to the macroscopic bagasse fibres, which leads to higher specific surface area. From the CNC thermal analysis the onset temperature for acid processed CNC occurred at 204 °C, which is much lower than for CNF and bagasse [8]. A similar reduction in degradation temperature was observed by Roman *et al* and it was concluded that remnant sulphate groups in the cellulose due to sulphuric acid treatment was found to be responsible for the reduced thermostability of the nanocrystals [16]. The elimination of sulphuric acid in sulfated anhydroglucose units required less energy [54], thus, during the thermal degradation process, sulphuric acid molecules could be released at much lower temperatures. The released sulphuric acid further facilitated the decomposition or depolymerisation of cellulose by removing some of the hydroxyl groups either by direct catalysis or esterification mechanisms. Moreover, smaller particles result in a large number of free end-chains where decomposition easily occurs
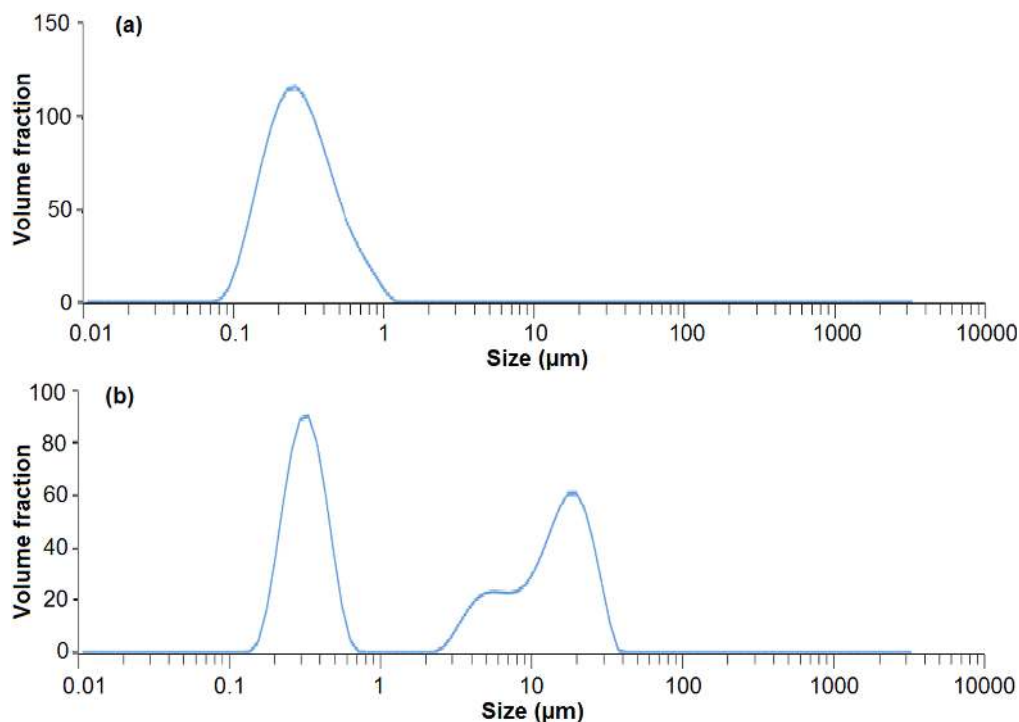

Figure 7. Size distribution of (a) CNC particle and (b) CNF particle.

Adv. Nat. Sci.: Nanosci. Nanotechnol. **7** (2016) 035004

M Rahimi Kord Sofla *et al*

[36, 55]. Briefly, the thermal analysis showed that the thermal degradation phenomenon of cellulose was initiated at a much lower temperature (204 °C), in the case of sulphuric acid processed nanocrystals while the CNF prepared by ball milling were not affected, indicating higher thermal stability. Similarly 50% weight loss occurred at 331 °C for CNF, which is much higher than the acid processed samples (260 °C). Thus it is inferred that CNF produced by the ball milling method retained the thermal stability of the native cellulose.

Moreover, the acid hydrolysed CNC sample has the highest residual mass at 600 °C. Nanocrystalline cellulose particles have a greater number of free end chains (produced during acid hydrolysis), due to their smaller particle size. The end chains start decomposition at a lower temperature [56] consequently causing an increase in the char yield of these hydrolysed samples [57]. Also, the sulphate groups introduced during hydrolysis with sulphuric acid could possibly act as a flame retardant [16].

3.6. Particle size measurement

The size distribution, as measured by DLS, of CNC is shown in figure 7(a), which shows that 90% of particles (by volume) are within the nano-scale range and the minimum particle size was ~100 nm. However, with ball milling, a wide bimodal distribution was observed (figure 7(b)). From figure 2, it is observed that some CNF structures are 10 μm in length but there are also some structures less than 1 μm which are due to breakage. Baheti *et al* postulated that the growth of a fibrous layer on the milling media (i.e. fibre coating the balls) decreased the potency of the impact force of the balls on the particles [58]. This results in some of the particles remaining as longer fibres in the micrometre range.

4. Conclusion

CNF and CNC were produced by ball milling and conventional acid hydrolysis respectively. Morphological analysis showed that CNC consists of uniform nanometre crystalline bundles, needle-like in shape with a low aspect ratio while CNF has longer lengths, higher aspect ratio and is less uniform. EDX results revealed small impurities in CNC because of residual sulphate groups from hydrolysis and small quantities of impurities in CNF came from residual bleaching agent. FTIR results confirm that following purification, cellulose, CNC and CNF, effectively all non-cellulosic material (i.e. hemicellulose and lignin) were removed as shown by the disappearance of the peak around 1700 cm^{-1}. It was found that CNC and CNF had a higher crystallite content compared to the bagasse raw material due to the removal of the hemicellulose and lignin. CNC had a higher crystalline fraction than CNF, which is attributed to the removal of the amorphous part of the microfibril during acid hydrolysis. Finally, the size distribution obtained by DLS revealed that ball milling resulted in micro and nanometer ranges of CNF, whereas acid hydrolysis leads to a uniform nanometre range for CNC.

References

[1] Gilfillan W N, Moghaddam L and Doherty W O 2014 *Cellulose* **21** 2695
[2] Mandal A and Chakrabarty D 2011 *Carbohyd. Polym.* **86** 1291
[3] Brinchi L, Cotana F, Fortunati E and Kenny J 2013 *Carbohyd. Polym.* **94** 154
[4] Leung A C, Lam E, Chong J, Hrapovic S and Luong J H 2013 *J. Nanopart. Res.* **15** 1
[5] Hsu L, Weder C and Rowan S J 2011 *J. Mater. Chem.* **21** 2812
[6] Okahisa Y, Yoshida A, Miyaguchi S and Yano H 2009 *Compos. Sci. Technol.* **69** 1958
[7] Fukuzumi H, Saito T, Iwata T, Kumamoto Y and Isogai A 2008 *Biomacromolecules* **10** 162
[8] Kelly J A, Shukaliak A M, Cheung C C, Shopsowitz K E, Hamad W Y and MacLachlan M J 2013 *Angew. Chem. Int. Ed.* **52** 8912
[9] Mendez J *et al* 2011 *Macromolecules* **44** 6827
[10] Walther A, Timonen J V, Díez I, Laukkanen A and Ikkala O 2011 *Adv. Mater.* **23** 2924
[11] Mendez J D and Weder C 2010 *Polym. Chem.* **1** 1237
[12] Nyström G, Razaq A, Strømme M, Nyholm L and Mihranyan A 2009 *Nano Lett.* **9** 3635
[13] Bondeson D, Mathew A and Oksman K 2006 *Cellulose* **13** 171
[14] Habibi Y, Lucia L A and Rojas O J 2010 *Chem. Rev.* **110** 3479
[15] Liu D, Chen X, Yue Y, Chen M and Wu Q 2011 *Carbohyd. Polym.* **84** 316
[16] Roman M and Winter W T 2004 *Biomacromolecules* **5** 1671
[17] Morais J P S, de Freitas Rosa M, Nascimento L D, do Nascimento D M and Cassales A R 2013 *Carbohyd. Polym.* **91** 229
[18] Boluk Y, Lahiji R, Zhao L and McDermott M T 2011 *Colloid. Surf.: Physicochem. Eng. Aspects* A **377** 297
[19] Morán J I, Alvarez V A, Cyras V P and Vázquez A 2008 *Cellulose* **15** 149
[20] Cherian B M *et al* 2011 *Carbohyd. Polym.* **86** 1790
[21] Rosa M *et al* 2010 *Carbohyd. Polym.* **81** 83
[22] Deepa B *et al* 2011 *Bioresource Technol.* **102** 1988
[23] Helbert W, Cavaille J and Dufresne A 1996 *Polym. Compos.* **17** 604
[24] Chen Y, Liu C, Chang P R, Cao X and Anderson D P 2009 *Carbohyd. Polym.* **76** 607
[25] Li R, Fei J, Cai Y, Li Y, Feng J and Yao J 2009 *Carbohyd. Polym.* **76** 94
[26] Bras J, Hassan M L, Bruzesse C, Hassan E A, El-Wakil N A and Dufresne A 2010 *Ind. Crop Prod.* **32** 627
[27] Nguyen H D, Mai T T T, Nguyen N B, Dang T D, Le M L P and Dang T T 2013 *Adv. Nat. Sci: Nanosci. Nanotechnol.* **4** 015016
[28] de Menezes A J, Siqueira G, Curvelo A A and Dufresne A 2009 *Polymer* **50** 4552
[29] Beck-Candanedo S, Roman M and Gray D G 2005 *Biomacromolecules* **6** 1048

[30] Zhang J, Elder T J, Pu Y and Ragauskas A J 2007 *Carbohyd. Polym.* **69** 607

[31] Zimmermann T, Bordeanu N and Strub E 2010 *Carbohyd. Polym.* **79** 1086

[32] Taniguchi T and Okamura K 1998 *Polym. Int.* **47** 291

[33] Chen W, Yu H, Liu Y, Chen P, Zhang M and Hai Y 2011 *Carbohyd. Polym.* **83** 1804

[34] Zhang L, Batchelor W, Varanasi S, Tsuzuki T and Wang X 2012 *Cellulose* **19** 561

[35] Chandel A K, da Silva S S, Carvalho W and Singh O V 2012 *J. Chem. Technol. Biot.* **87** 11

[36] Kumar A, Negi Y S, Choudhary V and Bhardwaj N K 2014 *J. Mater. Phys. Chem.* **2** 1

[37] Mwaikambo L Y and Ansell M P 2002 *J. Appl. Polym. Sci.* **84** 2222

[38] Segal L, Creely J, Martin A and Conrad C 1959 *Text. Res. J.* **29** 786

[39] Li J *et al* 2014 *Carbohyd. Polym.* **113** 388

[40] Khalil H, Ismail H, Rozman H and Ahmad M 2001 *Eur. Polym. J.* **37** 1037

[41] Nacos M *et al* 2006 *Carbohyd. Polym.* **66** 126

[42] Sain M and Panthapulakkal S 2006 *Ind. Crop. Prod.* **23** 1

[43] Li W *et al* 2014 *Carbohyd. Polym.* **113** 403

[44] Kumar A, Negi Y S, Bhardwaj N K and Choudhary V 2012 *Carbohyd. Polym.* **88** 1364

[45] Jonoobi M, Niska K O, Harun J and Misra M 2009 *BioResources* **4** 626

[46] Alemdar A and Sain M 2008 *Bioresource Technol.* **99** 1664

[47] Wu R-L, Wang X-L, Wang Y-Z, Bian X-C and Li F 2009 *Ind. Eng. Chem. Res.* **48** 7132

[48] de Souza Lima M M and Borsali R 2004 *Macromol. Rapid Comm.* **25** 771

[49] Nishiyama Y, Langan P and Chanzy H 2002 *J. Am. Chem. Soc.* **124** 9074

[50] Amiralian N, Annamalai P K, Memmott P and Martin D J 2015 *Cellulose* **22** 2483

[51] Kargarzadeh H, Ahmad I, Abdullah I, Dufresne A, Zainudin S Y and Sheltami R M 2012 *Cellulose* **19** 855

[52] Brown M E 2001 *Introduction to Thermal Analysis: Techniques and Applications* (Dordrecht: Springer Science & Business Media)

[53] Arbelaiz A, Fernandez B, Ramos J and Mondragon I 2006 *Thermochimica Acta* **440** 111

[54] Julien S, Chornet E and Overend R 1993 *J. Anal. Appl. Pyrol.* **27** 25

[55] Wang N, Ding E and Cheng R 2007 *Polymer* **48** 3486

[56] Staggs J 2006 *Polymer* **47** 897

[57] Piskorz J, Radlein D S A, Scott D S and Czernik S 1989 *J. Anal. Appl. Pyrol.* **16** 127

[58] Baheti V, Abbasi R and Militky J 2012 *World J. Eng.* **9** 45